TECHNICAL ARTICLE

Crystal structure of lacosamide form I, $C_{13}H_{18}N_2O_3$

James A. Kaduk,[1,a] Kai Zhong,[2] Amy M. Gindhart,[2] and Thomas N. Blanton[2]
[1]*Illinois Institute of Technology, 3101 S. Dearborn St., Chicago, Illinois 60616*
[2]*ICDD, 12 Campus Blvd., Newtown Square, Pennsylvania, 19073-3273*

(Received 9 March 2015; accepted 15 April 2015)

The crystal structure of lacosamide form I has been solved and refined using synchrotron X-ray powder diffraction data, and optimized using density functional techniques (density functional theory). Lacosamide form I crystallizes in space group $P2_1$ (#4) with $a = 10.677\,73(5)$, $b = 4.799\,68(2)$, $c = 13.639\,16(9)$ Å, $\beta = 91.6331(10)^\circ$, $V = 698.719(6)$ Å^3, and $Z = 2$. Van der Waals interactions are important in the crystal structure. Two N–H···O hydrogen bonds form C1,1(4) chains along the *b*-axis. Several weaker C–H···O hydrogen bonds to the ketone oxygens also contribute to the packing energy. These C–H···O extend both along the *b*-axis and in the *ac*-plane, and help link the molecules in three dimensions. The powder pattern has been submitted to International Centre for Diffraction Data for inclusion in the Powder Diffraction File™. © *2015 International Centre for Diffraction Data*.
[doi:10.1017/S0885715615000378]

Key words: lacosamide, Vimpat, powder diffraction, Rietveld refinement, density functional theory

I. INTRODUCTION

Lacosamide is an anticonvulsant drug useful in the treatment of central nervous system disorders such as epilepsy. The drug is also useful in the treatment of pain, especially diabetic neuropathic pain. Lacosamide is marketed under the trade name Vimpat® by Union Chimique Belge (UCB). It was approved by the Food and Drug Administration (FDA) as an adjunctive therapy for partial-onset seizures in 2008. Crystalline forms I and II, as well as amorphous lacosamide, are reported in US Patent 2009/0298947 (Mundorfer *et al.*, 2009), but no crystal structure has been reported. The systematic name (CAS Registry number 175481-36-4) is (*R*)-N-benzyl-2-acetamido-3-methoxypropionamide, and a two-dimensional (2D) molecular diagram is shown in Figure 1.

The presence of high-quality reference powder patterns in the Powder Diffraction File (PDF)® (ICDD, 2014) is important for phase identification, particularly by pharmaceutical, forensic, and law enforcement scientists. The crystal structures of a significant fraction of the largest dollar volume pharmaceuticals have not been published, and thus calculated powder patterns are not present in the PDF-4 databases. Sometimes experimental patterns are reported, but they are generally of low quality. This structure is the result of collaboration among International Centre for Diffraction Data (ICDD), Illinois Institute of Technology (IIT), Poly Crystallography Inc., and Argonne National Laboratory to measure high-quality synchrotron powder patterns of commercial pharmaceutical ingredients, include these reference patterns in the PDF, and determine the crystal structures of these Active Pharmaceutical Ingredients (APIs).

Even when the crystal structure of an API is reported, the single-crystal structure was often determined at low temperature. Most powder measurements are performed at ambient conditions. Thermal expansion (often anisotropic) means that the peak positions calculated from a low-temperature single-crystal structure often differ significantly from those measured at ambient conditions. These peak shifts can result in failure of default search/match algorithms to identify a phase, even when it is present in the sample. High-quality reference patterns measured at ambient conditions are thus critical for easy identification of APIs using standard powder diffraction practices.

II. EXPERIMENTAL

Lacosamide, a commercial reagent purchased from Carbosynth Company (Lot #FL248251201) was used as-received. The white powder was packed into a 1.5 mm diameter Kapton capillary, and rotated during the measurement at ~50 cycles s^{-1}. The powder pattern was measured at 295 K at beam line 11-BM (Lee *et al.*, 2008; Wang *et al.*, 2008) of the Advanced Photon Source at Argonne National Laboratory using a wavelength of 0.413 691 Å from 0.5° to 50° 2θ with a step size of 0.001° and a counting time of 0.1 s step^{-1}. The pattern was indexed on a primitive monoclinic unit cell having $a = 13.634$, $b = 4.799$, $c = 10.670$ Å, $\beta = 91.7^\circ$, $V = 679.9$ Å^3, and $Z = 2$ using Jade 9.5 (MDI, 2014).

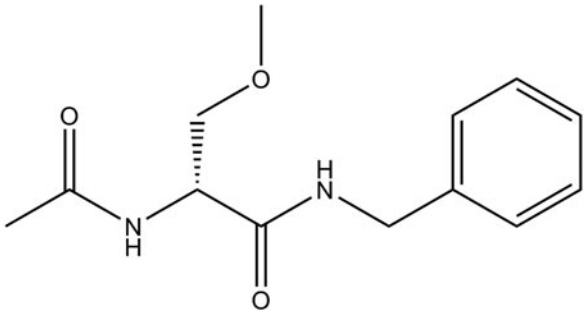

Figure 1. The molecular structure of lacosamide.

[a]Author to whom correspondence should be addressed. Electronic mail: kaduk@polycrystallography.com

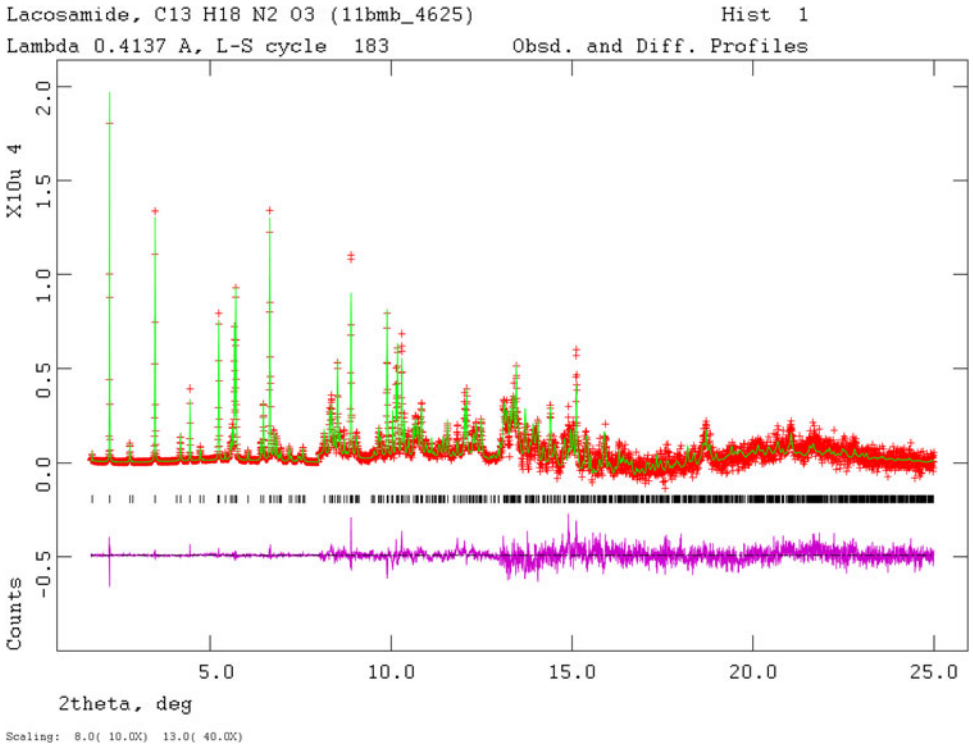

Figure 2. (Color online) The Rietveld plot for the refinement of lacosamide form I. The red crosses represent the observed data points, and the green line is the calculated pattern. The magenta curve is the difference pattern, plotted at the same vertical scale as the other patterns. The vertical scale has been multiplied by a factor of 10 for $2\theta > 8.0^{\circ}$, and by a factor of 40 for $2\theta > 13.0^{\circ}$.

An analysis of systematic absences using EXPO2013 (Altomare *et al.*, 2013) suggested that the space group was $P2_1$ (#4), which was confirmed by successful solution and refinement of the structure. Although both $P2_1$ and $P2_1/m$ have the same systematic absences, the fact that lacosamide is a chiral molecule requires the space group to be $P2_1$. A reduced cell search in the Cambridge Structural Database (Allen, 2002) yielded 15 hits, but no structure for lacosamide.

A lacosamide molecule was built and its conformation optimized using Spartan '14 (Wavefunction, 2013), and saved as a mol2 file. This file was converted into a Fenske–Hall *Z*-matrix file using OpenBabel (O'Boyle *et al.*, 2011). This molecule was used to solve the structure with FOX (Favre-Nicolin and Černý, 2002). The maximum $\sin\theta/\lambda$ used in the solution was 0.40 Å^{-1}. Initial positions of the active hydrogens were deduced by the analysis of potential hydrogen-bonding patterns.

Rietveld refinement was carried out using the General Structure Analysis System (GSAS, Larson and Von Dreele, 2004). Only the 1.7°–25.0° portion of the pattern was included in the refinement ($d_{\min} = 0.95$ Å). The C1–H11 phenyl group was refined as a rigid body. All other non-H bond distances and angles were subjected to restraints, based on a Mercury/Mogul Geometry Check (Sykes *et al.*, 2011; Bruno *et al.*, 2004) of the molecule. The Mogul average and standard deviation for each quantity were used as the restraint parameters. The restraints contributed 3.16% to the final χ^2. Isotropic displacement coefficients were refined, and grouped by chemical similarity. The hydrogen atoms were included in calculated positions, which were recalculated during the refinement. The U_{iso} of each hydrogen atom was constrained to be 1.3× that of the heavy atom to which it is attached. The peak profiles were described using profile function #4 (Thompson *et al.*, 1987; Finger *et al.*, 1994), which includes the Stephens (1999) anisotropic strain broadening model. The background was modeled using a three-term shifted Chebyshev polynomial, with an eight-term diffuse scattering function to model the Kapton capillary and any amorphous component. The final refinement of 78 variables using 23 330 observations (23 302 data points and 28 restraints) yielded the residuals $R_{wp} = 0.069$, $R_p = 0.054$, and $\chi^2 = 1.392$. The largest peak (1.37 Å from C12) and hole (2.13 Å from C20) in the difference Fourier map were 0.28 and −0.26 *e* (Å^{-3}), respectively. The Rietveld plot is included as Figure 2. The largest errors are in the shapes of some of the low-angle peaks, and may indicate subtle changes in the sample during the measurement. These features persist in a Le Bail fit of the pattern ($\chi^2 = 1.12$), especially in the strong 100 peak at low angle.

A density functional geometry optimization (fixed experimental unit cell) was carried out using CRYSTAL09 (Dovesi *et al.*, 2005). The basis sets for the H, C, and O atoms were those of Gatti *et al.* (1994). The calculation used eight *k*-points and the B3LYP functional, and took ~6 days on a 3.0 GHz PC.

III. RESULTS AND DISCUSSION

The powder pattern corresponds to that of form I of lacosamide, as described by Mundorfer *et al.* (2009), so the crystal structure reported here is that of form I. The refined atom coordinates of lacosamide are reported in Table I, and the coordinates from the density functional theory (DFT) optimization in Table II. The root-mean-square deviation of the

https://doi.org/10.1017/S0885715615000378 Published online by Cambridge University Press

TABLE I. Rietveld refined crystal structure of lacosamide form I.

Crystal data	
$C_{13}H_{18}N_2O_3$	$\beta = 91.6331\ (10)^\circ$
$M_w = 250.30$	$V = 698.719\ (6)$ Å^3
Monoclinic, $P2_1$	$Z = 2$
$a = 10.677\ 73\ (5)$ Å	Synchrotron radiation, $\lambda = 0.413\ 691$ Å
$b = 4.799\ 68\ (2)$ Å	$T = 295$ K
$c = 13.639\ 16\ (9)$ Å	Cylinder, 1.5×1.5 mm
Data collection	
11-BM APS diffractometer	Scan method: step
Specimen mounting: Kapton capillary	$2\theta_{min} = 0.5^\circ$, $2\theta_{max} = 50.0^\circ$, $2\theta_{step} = 0.001^\circ$
Data collection mode: transmission	
Refinement	
Least-squares matrix: full	23302 data points
$R_p = 0.054$	Profile function: CW Profile function number 4 with 21 terms Pseudo Voigt profile coefficients as parameterized in Thompson *et al.* (1987). Asymmetry correction of Finger *et al.* (1994). Microstrain broadening by Stephens (1999). #1(GU) = 47.730 #2(GV) = −0.126 #3(GW) = 0.063 #4(GP) = 0.000 #5(LX) = 0.173 #6(ptec) = 0.00 #7(trns) = 0.00 #8(shft) = 0.0000 #9(sfec) = 0.00 #10(S/L) = 0.0011 #11(H/L) = 0.0011 #12(eta) = 0.8589 #13(S400) = 2.6×10^{-2} #14(S040) = 3.8×10^{-1} #15(S004) = 2.0×10^{-2} #16(S220) = 2.3×10^{-2} #17(S202) = 1.7×10^{-1} #18(S022) = 3.3×10^{-1} #19(S301) = -1.2×10^{-2} #20(S103) = 1.3×10^{-2} #21(S121) = -9.7×10^{-2} Peak tails are ignored where the intensity is below 0.0010 times the peak Aniso. broadening axis 0.0 0.0 1.0
$R_{wp} = 0.069$	78 parameters
$R_{exp} = 0.060$	28 restraints
$R(F^2) = 0.103\ 26$	$(\Delta/\sigma)_{max} = 0.03$
$\chi^2 = 1.392$	Background function: GSAS Background function number 1 with 3 terms. Shifted Chebyshev function of first kind 1: 126.222 2: 14.2595 3: −17.5494

Fractional atomic coordinates and isotropic displacement parameters (Å^2)

	x	y	z	U_{iso}
C1	0.9085 (3)	0.7416 (8)	0.2821 (3)	0.0927 (14)
C2	0.9690 (4)	0.8966 (9)	0.355 61 (18)	0.0927 (14)
C3	1.0642 (4)	1.0810 (9)	0.3320 (3)	0.0927 (14)
C4	1.0989 (3)	1.1104 (10)	0.2350 (3)	0.0927 (14)
C5	1.0384 (4)	0.9554 (13)	0.1615 (2)	0.0927 (14)
C6	0.9432 (4)	0.7710 (12)	0.1851 (2)	0.0927 (14)
H7	0.9451 (6)	0.8763 (12)	0.4225 (2)	0.1205 (18)
H8	1.1059 (5)	1.1878 (12)	0.3827 (4)	0.1205 (18)
H9	1.1741 (4)	1.2561 (12)	0.2163 (5)	0.1205 (18)
H10	1.0623 (7)	0.9757 (17)	0.0946 (2)	0.1205 (18)
H11	0.9015 (6)	0.6642 (15)	0.1344 (3)	0.1205 (18)
C12	0.8029 (4)	0.559 68	0.3067 (4)	0.0480 (11)
N13	0.6834 (3)	0.6651 (7)	0.2696 (4)	0.0480 (11)
C14	0.5889 (3)	0.4967 (10)	0.2500 (4)	0.0480 (11)
O15	0.5990 (3)	0.2429 (10)	0.2563 (4)	0.0480 (11)
C16	0.4637 (3)	0.6281 (11)	0.2322 (3)	0.0480 (11)
N17	0.4106 (4)	0.5271 (10)	0.1410 (3)	0.0498 (9)
C18	0.3674 (6)	0.6923 (10)	0.0726 (3)	0.0498 (9)
O19	0.3592 (4)	0.9454 (10)	0.0851 (3)	0.0498 (9)
C20	0.3136 (6)	0.5507 (12)	−0.0174 (4)	0.0498 (9)
C21	0.3797 (5)	0.5532 (14)	0.3152 (3)	0.0498 (9)
O22	0.4187 (4)	0.6979 (13)	0.4006 (3)	0.0498 (9)
C23	0.3569 (6)	0.5976 (12)	0.4814 (4)	0.0498 (9)
H24	0.798 21	0.531 04	0.387 92	0.0624 (15)
H25	0.813 62	0.347 68	0.269 18	0.0624 (15)
H26	0.665 22	0.895 99	0.261 97	0.0624 (15)
H27	0.473 13	0.871 28	0.233 23	0.0624 (15)
H28	0.400 62	0.316 76	0.127 25	0.0648 (12)
H29	0.33015	0.327 08	−0.006 56	0.0648 (12)
H30	0.346 03	0.646 17	−0.082 79	0.0648 (12)
H31	0.202 56	0.591 51	−0.010 79	0.0648 (12)
H32	0.378 46	0.320 02	0.324 85	0.0648 (12)
H33	0.278 39	0.629 54	0.296 24	0.0648 (12)
H34	0.373 32	0.350 16	0.486 11	0.0648 (12)
H35	0.255 37	0.633 32	0.470 02	0.0648 (12)
H36	0.397 57	0.689 95	0.549 67	0.0648 (12)

https://doi.org/10.1017/S0885715615000378 Published online by Cambridge University Press

TABLE II. DFT-optimized (CRYSTAL09) crystal structure of lacosamide form I.

Crystal data	
$C_{13}H_{18}N_2O_3$	$\beta = 91.6331°$
$M_w = 250.30$	$V = 698.72\ (1)$ Å^3
Monoclinic, $P2_1$	$Z = 2$
$a = 10.6777$ Å	
$b = 4.7997$ Å	
$c = 13.6392$ Å	

Fractional atomic coordinates and isotropic displacement parameters (Å^2)

	x	y	z	U_{iso}
C1	0.912 83	0.760 17	0.277 64	0.0927
C2	0.990 42	0.924 80	0.338 26	0.0927
C3	1.088 21	1.078 89	0.299 14	0.0927
C4	1.109 56	1.069 27	0.198 78	0.0927
C5	1.032 32	0.905 07	0.137 73	0.0927
C6	0.934 67	0.752 17	0.176 82	0.0927
H7	0.974 26	0.932 99	0.416 62	0.1205
H8	1.147 42	1.206 93	0.346 92	0.1205
H9	1.186 60	1.183 89	0.168 12	0.1205
H10	1.048 78	0.895 27	0.059 58	0.1205
H11	0.875 02	0.623 67	0.129 42	0.1205
C12	0.808 05	0.590 63	0.320 02	0.048
N13	0.684 86	0.682 26	0.284 14	0.048
C14	0.592 33	0.504 02	0.260 22	0.048
O15	0.604 40	0.246 36	0.260 51	0.048
C16	0.464 54	0.633 01	0.234 16	0.048
N17	0.416 99	0.527 14	0.140 53	0.0498
C18	0.371 15	0.698 11	0.068 99	0.0498
O19	0.370 37	0.955 61	0.077 34	0.0498
C20	0.317 33	0.557 47	−0.021 92	0.0498
C21	0.373 80	0.559 80	0.315 59	0.0498
O22	0.421 53	0.674 79	0.404 46	0.0498
C23	0.355 45	0.582 71	0.487 03	0.0498
H24	0.812 99	0.604 16	0.400 40	0.0624
H25	0.817 48	0.370 98	0.300 65	0.0624
H26	0.666 35	0.890 62	0.281 67	0.0624
H27	0.472 30	0.858 50	0.228 25	0.0624
H28	0.414 51	0.317 04	0.129 36	0.0648
H29	0.330 68	0.332 37	−0.020 75	0.0648
H30	0.359 58	0.646 93	−0.086 70	0.0648
H31	0.216 86	0.602 81	−0.027 19	0.0648
H32	0.366 08	0.331 56	0.321 35	0.0648
H33	0.280 81	0.645 06	0.296 02	0.0648
H34	0.364 66	0.356 34	0.496 92	0.0648
H35	0.255 29	0.637 28	0.480 01	0.0648
H36	0.396 94	0.684 59	0.551 55	0.0648

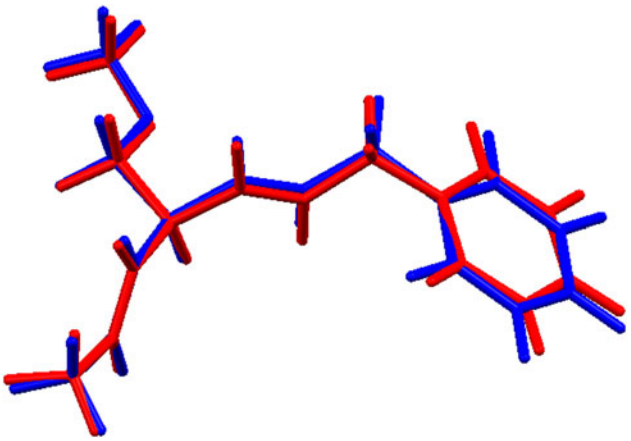

Figure 3. (Color online) Comparison of the refined and optimized structures of lacosamide. The Rietveld refined structure is colored red, and the DFT-optimized structure is in blue.

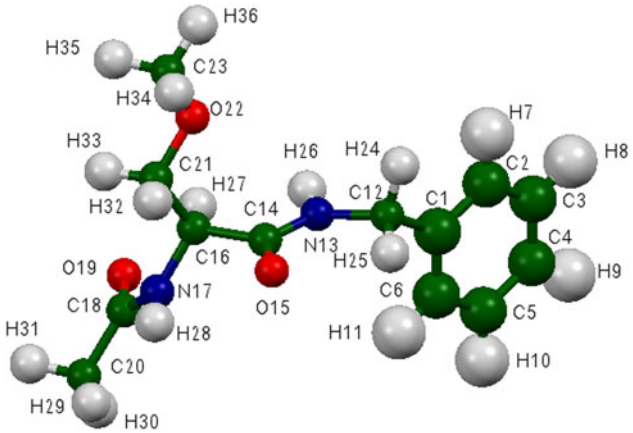

Figure 4. (Color online) The molecular structure of lacosamide, with the atom numbering. The atoms are represented by 50% probability spheroids.

https://doi.org/10.1017/S0885715615000378 Published online by Cambridge University Press

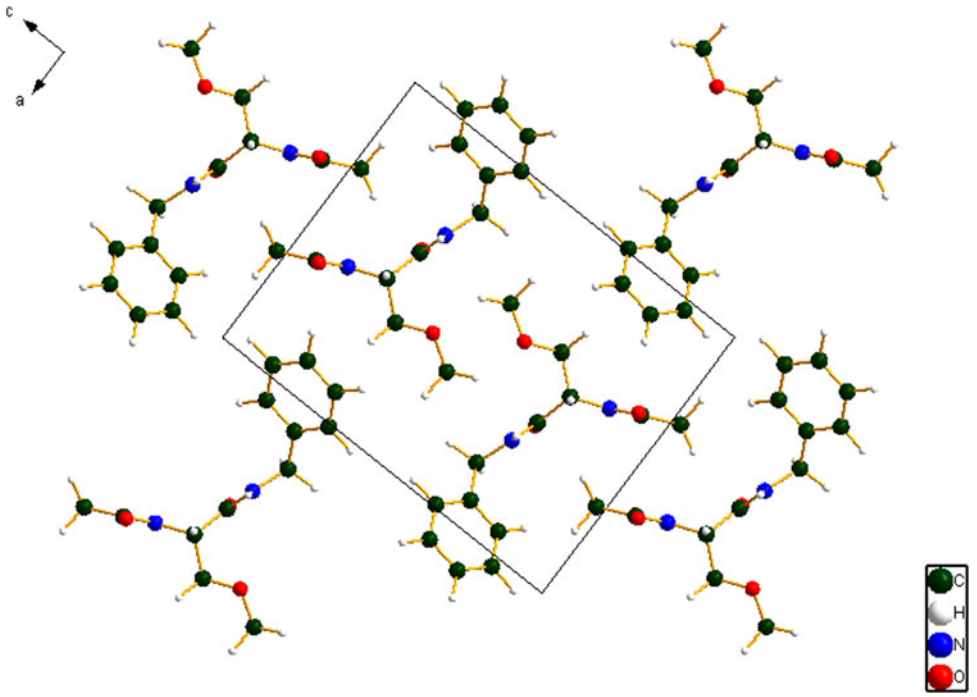

Figure 5. (Color online) The crystal structure of lacosamide form I, viewed down the *b*-axis. The hydrogen bonds are shown as dashed lines.

non-hydrogen atoms is 0.195 Å, and the maximum deviation is 0.302 Å, at several atoms (Figure 3). The good agreement between the refined and optimized structures is strong evidence that the structure is correct (van de Streek and Neumann, 2014). The discussion of the geometry uses the DFT-optimized structure. The asymmetric unit (with atom numbering) is illustrated in Figure 4, and the crystal structure is presented in Figure 5.

All of the bond distances, bond angles, and torsion angles fall within the normal ranges indicated by a Mercury Mogul Geometry Check (Macrae *et al.*, 2008). A quantum mechanical conformation examination (DFT/B3LYP/6-31G*/water) using Spartan '14 indicated that the observed conformation is ~2.6 kcal mole^{-1} higher in energy than a local minimum. A molecular mechanics force field (MMFF) sampling of conformational space indicated that the solid-state conformation is 49.0 kcal mole^{-1} higher in energy than the minimum energy conformation, which has a much more compact geometry. The energy difference indicates that van der Waals forces contribute significantly to the crystal energy.

Analysis of the contributions to the total crystal energy using the Forcite module of Materials Studio (Accelrys, 2013) suggests that the intramolecular deformation energy is small, and is equally distributed among bond, angle, and torsion angle distortion terms. The intermolecular energy is dominated by electrostatic contributions, which in this force-field-based analysis include hydrogen bonds, although van der Waals attraction is also significant. The van der Waals interactions presumably result from the parallel stacking of phenyl rings. The hydrogen bonds are better analyzed using the results of the DFT calculation.

Prominent in the crystal structure are the two hydrogen bonds N13–H26···O15 and N17–H28···O19 (Table III). Each of these forms a chain with a graph set (Etter, 1990; Bernstein *et al.*, 1995; Shields *et al.*, 2000) C1,1(4). These patterns combine into several more-complex chain and ring patterns. The hydrogen bond chains run parallel to the *b*-axis. Several weaker C–H···O hydrogen bonds to the ketone oxygens also contribute to the packing energy. These C–H···O extend both along the *b*-axis and in the *ac*-plane, and help link the molecules in three dimensions (Figure 6). The crystal consists of hydrophobic and hydrophilic regions.

The volume enclosed by the Hirshfeld surface (Figure 7; Hirshfeld, 1977; McKinnon *et al.*, 2004; Spackman and Jayatilaka, 2009; Wolff *et al.*, 2012) is 342.32 Å^3, 98.0% of ½ the unit cell volume. The molecules are thus not tightly packed. The only significant close contacts (red in Figure 6) involve the hydrogen bonds.

TABLE III. Hydrogen bonds in the DFT-optimized crystal structure of lacosamide form I.

D–H···*A*	D–H (Å)	H···A (Å)	D···A (Å)	D–H···Å	Overlap (*e*)
N13–H26···O15	1.02	1.851	2.856	167.9	0.055
N17–H28···O19	1.02	1.928	2.914	161.7	0.049
C12–H25···O15	1.092	2.401	2.831	101.7	0.014
C16–H27···O19	1.089	2.347	2.804	103.2	0.014
C20–H29···O19	1.09	2.282	3.233	144.7	0.026
C20–H30···O15	1.091	2.459	3.502	159.4	0.014
C23–H36···O15	1.09	2.581	3.546	147.1	0.011

https://doi.org/10.1017/S0885715615000378 Published online by Cambridge University Press

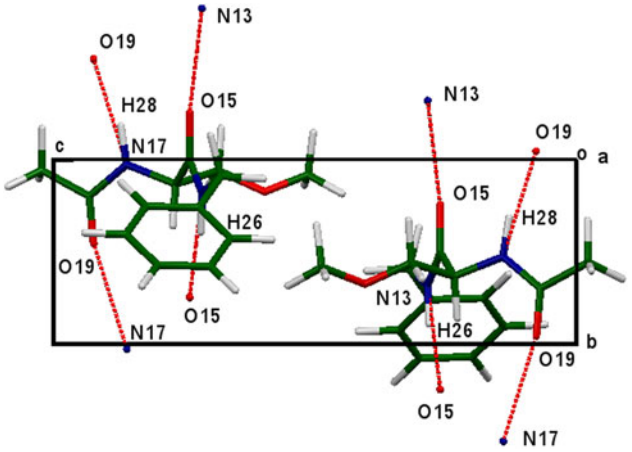

Figure 6. (Color online) A view of the lacosamide form I structure, viewed down the *a*-axis to illustrate the hydrogen bonds.

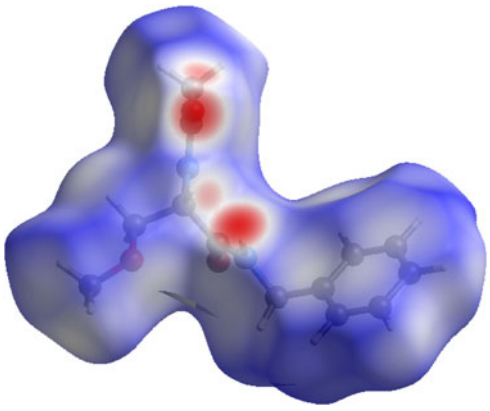

Figure 7. (Color online) The Hirshfeld surface of lacosamide. Intermolecular contacts longer than the sums of the van der Waals radii are colored blue, and contacts shorter than the sums of the radii are colored red. Contacts equal to the sums of the radii are white.

The Bravais–Friedel–Donnay–Harker (Bravais, 1866; Friedel, 1907; Donnay and Harker, 1937) morphology suggests that we might expect a needle-like morphology for lacosamide form I, with <010> as the long axis, or perhaps platy morphology with {001} as the principal faces. A fourth-order spherical harmonic preferred orientation model was included in the refinement; the texture index was 1.076, indicating that preferred orientation was modest in this rotated capillary specimen. The powder pattern of lacosamide form I has been submitted to ICDD for inclusion in the PDF.

ACKNOWLEDGEMENTS

Use of the Advanced Photon Source at Argonne National Laboratory was supported by the U. S. Department of Energy, Office of Science, Office of Basic Energy Sciences, under Contract No. DE-AC02-06CH11357. This work was partially supported by the International Centre for Diffraction Data. The authors thank Lynn Ribaud for his assistance in data collection.

SUPPLEMENTARY MATERIALS AND METHODS

The supplementary material for this article can be found at http://www.journals.cambridge.org/PDJ

Accelrys (**2013**). *Materials Studio 7.0* (Accelrys Software Inc., San Diego, CA).

Allen, F. H. (**2002**). "The Cambridge structural database: a quarter of a million crystal structures and rising," Acta Crystallogr. Sect. B: Struct. Sci. **58**, 380–388.

Altomare, A., Cuocci, C., Giacovazzo, C., Moliterni, A., Rizzi, R., Corriero, N. and Falcicchio, A. (**2013**). "EXPO2013: a kit of tools for phasing crystal structures from powder data," J. Appl. Crystallogr. **46**, 1231–1235.

Bernstein, J., Davis, R. E., Shimoni, L., and Chang, N. L. (**1995**). "Patterns in hydrogen bonding: functionality and graph set analysis in crystals," Angew. Chem. Int. Ed. Engl. **34**(15), 1555–1573.

Bravais, A. (**1866**). *Etudes Cristallographiques* (Gauthier Villars, Paris).

Bruno, I. J., Cole, J. C., Kessler, M., Luo, J., Motherwell, W. D. S., Purkis, L. H., Smith, B. R., Taylor, R., Cooper, R. I., Harris, S. E., and Orpen, A. G. (**2004**). "Retrieval of crystallographically-derived molecular geometry information," J. Chem. Inf. Comput. Sci. **44**, 2133–2144.

Donnay, J. D. H., and Harker, D. (**1937**). "A new law of crystal morphology extending the law of Bravais," Amer. Mineral. **22**, 446–467.

Dovesi, R., Orlando, R., Civalleri, B., Roetti, C., Saunders, V. R., and Zicovich-Wilson, C. M. (**2005**). "CRYSTAL: a computational tool for the *ab initio* study of the electronic properties of crystals," Z. Kristallogr. **220**, 571–573.

Etter, M. C. (**1990**). "Encoding and decoding hydrogen-bond patterns of organic compounds," Acc. Chem. Res. **23**(4), 120–126.

Favre-Nicolin, V., and Černý, R. (**2002**). "FOX, Free objects for crystallography: a modular approach to ab initio structure determination from powder diffraction," J. Appl. Crystallogr. **35**, 734–743.

Finger, L. W., Cox, D. E., and Jephcoat, A. P. (**1994**). "A correction for powder diffraction peak asymmetry due to axial divergence," J. Appl. Crystallogr. **27**(6), 892–900.

Friedel, G. (**1907**). "Etudes sur la loi de Bravais," Bull. Soc. Fr. Mineral. **30**, 326–455.

Gatti, C., Saunders, V. R., and Roetti, C. (**1994**). "Crystal-field effects on the topological properties of the electron-density in molecular crystals – the case of urea," J. Chem. Phys. **101**, 10686–10696.

Hirshfeld, F. L. (**1977**). "Bonded-atom fragments for describing molecular charge densities," Theor. Chem. Acta **44**, 129–138.

ICDD (**2014**). "PDF-4+ 2014 (Database)," in *International Centre for Diffraction Data*, edited by Dr. Soorya Kabekkodu (Newtown Square, PA, USA).

Larson, A. C., and Von Dreele, R. B. (**2004**). General Structure Analysis System, (GSAS), Los Alamos National Laboratory Report LAUR 86-784.

Lee, P. L., Shu, D., Ramanathan, M., Preissner, C., Wang, J., Beno, M. A., Von Dreele, R. B., Ribaud, L., Kurtz, C., Antao, S. M., Jiao, X., and Toby, B. H. (**2008**). "A twelve-analyzer detector system for high-resolution powder diffraction," J. Synchroton. Radiat. **15**(5), 427–432.

Macrae, C. F., Bruno, I. J., Chisholm, J. A., Edington, P. R., McCabe, P., Pidcock, E., Rodriguez-Monge, L., Taylor, R., van de Streek, J., and Wood, P. A. (**2008**). "Mercury CSD 2.0 – new features for the visualization and investigation of crystal structures," J. Appl. Crystallogr. **41**, 466–470.

McKinnon, J. J., Spackman, M. A., and Mitchell, A. S. (**2004**). "Novel tools for visualizing and exploring intermolecular interactions in molecular crystals," Acta Crystallogr. Sect. B **60**, 627–668.

MDI (**2014**). *Jade 9.5* (Materials Data. Inc., Livermore CA).

Mundorfer, T., Markovic, M., Kosutic Hulita, N., and Zegarac, M. (**2009**). "Polymorphic and Amorphous Forms of Lacosamide and Amorphous Compositions," U.S. Patent 2009/0298947.

O'Boyle, N. M., Banck, M., James, C. A., Morley, C., Vandermeersch, T., and Hutchison, G. R. (**2011**). "Open Babel: An open chemical toolbox," J. Chem. Inf. **3**(33); DOI:10.1186/1758-2946-3-33.

Shields, G. P., Raithby, P. R., Allen, F. H., and Motherwell, W. S. (**2000**). "The assignment and validation of metal oxidation states in the Cambridge Structural Database," Acta Crystallogr. Sec. B: Struct. Sci. **56**(3), 455–465.

Spackman, M. A., and Jayatilaka, D. (**2009**). "Hirshfeld surface analysis," CrystEngComm. **11**, 19–32.

Stephens, P. W. (**1999**). "Phenomenological model of anisotropic peak broadening in powder diffraction," J. Appl. Crystallogr. **32**, 281–289.

Sykes, R. A., McCabe, P., Allen, F. H., Battle, G. M., Bruno, I. J., and Wood, P. A. (**2011**). "New software for statistical analysis of Cambridge Structural Database data," J. Appl. Crystallogr. **44**, 882–886.

Thompson, P., Cox, D. E., and Hastings, J. B. (**1987**). "Rietveld refinement of Debye-Scherrer synchrotron X-ray data from Al_2O_3," J. Appl. Crystallogr. **20**(2), 79–83.

van de Streek, J. and Neumann, M. A. (**2014**). "Validation of molecular crystal structures from powder diffraction data with dispersion-corrected density functional theory (DFT-D)," Acta Crystallogr. Sect. B: Struct. Sci. **70**(6), 1020–1032.

Wang, J., Toby, B. H., Lee, P. L., Ribaud, L., Antao, S. M., Kurtz, C., Ramanathan, M., Von Dreele, R. B., and Beno, M. A. (**2008**). "A dedicated powder diffraction beamline at the advanced photon source: commissioning and early operational results," Rev. Sci. Instrum. **79**, 085105.

Wavefunction, Inc. (**2013**). *Spartan '14 Version 1.1.0* (Wavefunction Inc., Irvine CA).

Wolff, S. K., Grimwood, D. J., McKinnon, M. J., Turner, M. J., Jayatilaka, D., and Spackman, M. A. (**2012**). CrystalExplorer Version 3.1, (University of Western Australia).

https://doi.org/10.1017/S0885715615000378 Published online by Cambridge University Press